Original Article

Highly Efficient Base-Catalyzed Synthesisof Piperidine-4-Imine Lead Molecules For SARS-Cov-2 Mutant Spike Proteasevia In Silico Method

K.Sadhana[1], M.Premalatha[2], Dr. S. Aruna[3]*,Sathiskumar Udayasan[4],Dr. M.Saamanthi[5]

[1]Tamil Nadu Pollution Control Board, Maraimalainagar, Chengalpet.
[4]Adhi College of Engineering & Technology
[2,3] PG & Research Department of chemistry, Queen Mary's College, Chennai- 600004,India
Department of chemistry, Don Bosco College, Dharmapuri
DOI: 10.47750/pnr.2022.13.S09.448

Abstract

For the discovery of drugs to SARS-CoV-2 pandemics, we have developed a new series of piperidine-4-imines as the central core owing to significant pharmaceuticaldemands on it. The synthesis of piperidine-4-imines involvesatwo-step base-catalyzed reaction, namely (i)condensations followed by cyclization with aromatic aldehyde, aliphatic ketone, and ammonia to yield piperidine-4-ketone core, and (ii) a simple Schiff base/piperidine-4-imines formation between piperidine-4-ketone andvarious aromatic primary amines. All the synthesized intermediate and target piperidine-4-imines molecular structures were well characterized by NMR, FT-IR, and mass spectral studies.

Further, the ground state geometry of synthesized molecules was optimized using density function theory (DFT) with basis set of b3lyp 6-31g (d,p) in Gaussian 09 program. Using this molecular geometry, we docked against SARS-CoV-2 mutant spike protease of delta, delta plus, and omicron, which shows an effective binding ability. In addition, Lipinski's rule, pre ADME and toxicity studies also reveal drug-likeness properties.

Keywords: Piperidine-4-imine, Base-catalyzed, SARS-Cov-2, Density functional theory, and Docking.

1. Introduction:

In 2019 onwards, the so-called term 'coronavirus' has transmitted very fast from human-to-human via aerosols and lead to many sudden deaths from China, a city in Wuhan. [1,2] Later, this life-threatening corona viral disease gradually spread throughout the world. Therefore, global emergency was made on 11 Feb 2020 through the International Virus Classification Commission (ICTV) to categorize this new coronavirus as '2019-nCoV'. Meanwhile, the World Health Organization (WHO) also named the 2019-nCoV as 'COVID-19'[3]. The pandemic waves lead to severe acute respiratory syndrome and other chronic illnesses to the affected human regardless of age. Later, the COVID-19 was resolved as 'severe acute respiratory syndrome coronavirus-2' (SARS-CoV-2)[4]. An outbreak of the SARS-CoV-2 seems completely unable to stop or control because of the improper social distance all over the affected countries. Therefore,the pandemic distribution rate drastically increased by infected or asymptomatic patients via aerosols. Typically, symptoms of the SARS-CoV-2 include cough, fever, breathing difficulty, sore throat, diarrhea, headache, nausea, congestion, and loss of taste, leading to severe respiratory problems and finally to death[5,6]. Hence, the SARS-CoV-2 is now called a 'novel coronavirus'[7]. In SARS-CoV-2, the spike receptor protease plays a critical role, which facilitates the virus invasion on the human cell receptor (angiotension converting enzyme-2, ACE2) and the host cell

receptor (transmembrane protease serine-2, TMPRSS2)[8]. Furthermore, the pandemic is quickly shifted to second waves of delta (variant B.1.617) and delta plus (variant 1.617.2), and then third waves of omicron (variant B.1.1.529)[9,10,11].The WHO statistically reports that the global pandemic distribution rate is 53,75,91,764 confirmed cases as of 21 June 2022. Amongst them, 63,19,395 people have died in overall 223 countries. To overcome this situation, several researchershave suggested some of the repurposing small-molecule based antiviral drugs such as Remdesivir[12], hydroxychloroquine[13], favipiravir[14], pirfenidone[15], and lopinavir/ritonavir[16] for the effective treatment of SARS CoV-2 and its mutations. Unexpectedly, none of these drugs could effectively cure the completely. Also, they cause several side effects on post-COVID-19 treatment. Hence, the development of potential drugs is highly warranted.

In our drug discovery program, we focused on piperidine-4-imines,which arenaturally occurring bioactive compounds and having two nitrogen atoms including exocyclic imines. They possess significant biological properties foracting as anti-viral,[17] anti-microbial,[18]anti-inflammatory,[19] anti-cancer,[20]and anti-anxiety[21] agents. Among the piperidine-4-imines, N-benzhydrylpiperidine-4-amine derivatives exhibit a promising class of interest to anti-microbial (Bacillus subtilis, Escherichia coli, Klebsiella pneumonia, and Streptococcus aureus)[21] and anti-fungal activities(Aspergillusniger, Aspergillusflavus, and fungi.).[22] A series of novel piperidine-4-imine derivatives show anti-tubercular agents against Mycobacterium tuberculosisH37Rv.[23]Similarly, Ghosh et al. developed a nitrogen-containing five-membered ring with chloropyridinyl derivatives for SARS-CoV-2.[24]Very recently, Pfizer have developed a nitrogen heterocyclic drug toinhibitingthe coronavirus 3CL protease for the potential treatment of COVID-19.[25]

Indeed, there is no selective anti-viral drug discovered against SARS-CoV-2 and its various mutations so far. This accelerates us to develop a novel and potential piperidine-4-imine-based anti-viral compounds for SARS CoV-2, delta, delta plus, and omicron. The synthesized lead molecules undergone complete experimental spectroscopic investigationssuch as FT-IR, NMR, and mass spectral analyses. Also, theoretical computations DFT/B3LYP method and6-31g (d, p) basis set were used to optimize the ground state structures. Finally, the binding ability of the lead molecules wasdetermined using AutodockVina. In addition, the drug-likeness properties were calculated by online preADME software.

2. Results and discussion:

Here, we have synthesized a series of novel piperidine-4-imines via two-step reactions as shown in **Fig. 1.**Initially,a classical multi-component reaction of Petrenko-Kritschenko piperidin-4-one synthesis involved a ring-condensation of octan-3-one(**1**), 3,4,5-trimethoxy benzaldehyde (**2**) and ammonia in water medium to yield 88% as solid.Later, the synthesized piperidin-4-one precursor reactswith substituted aromatic primary amines offering a novel piperidin-4-ones as solid with 78% yield. The overall products were obtained in the range of 65to 75% yields.

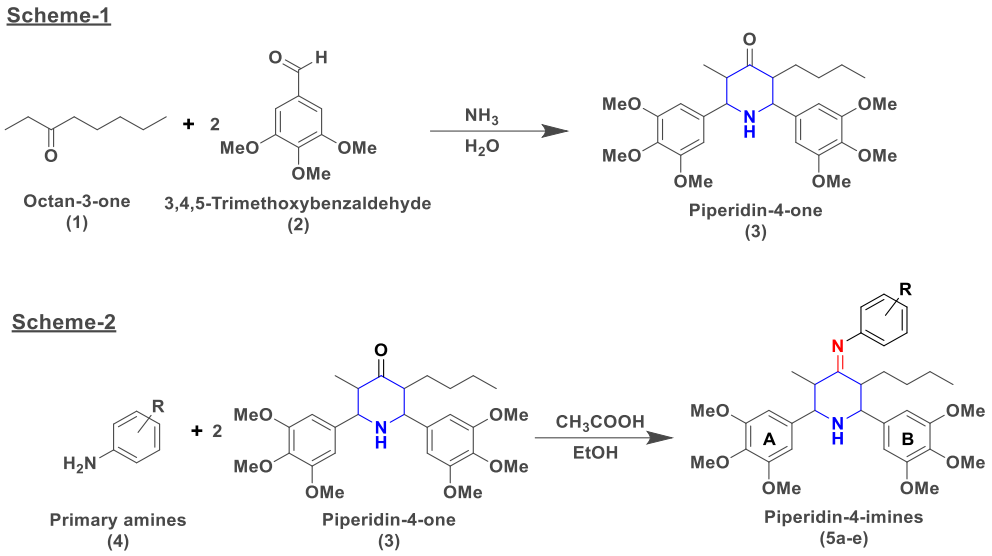

Fig. 1.Synthesis of piperidin-4-imines

Using piperidin-4-one, five piperidin-4-imines (**5a-e**) have been synthesized as shown in **Chart 1.**All the synthesized compounds and precursor molecular structures were well characterized by HR-MS, NMR, and FT-IR spectroscopic data.

3. Density Functional Theory

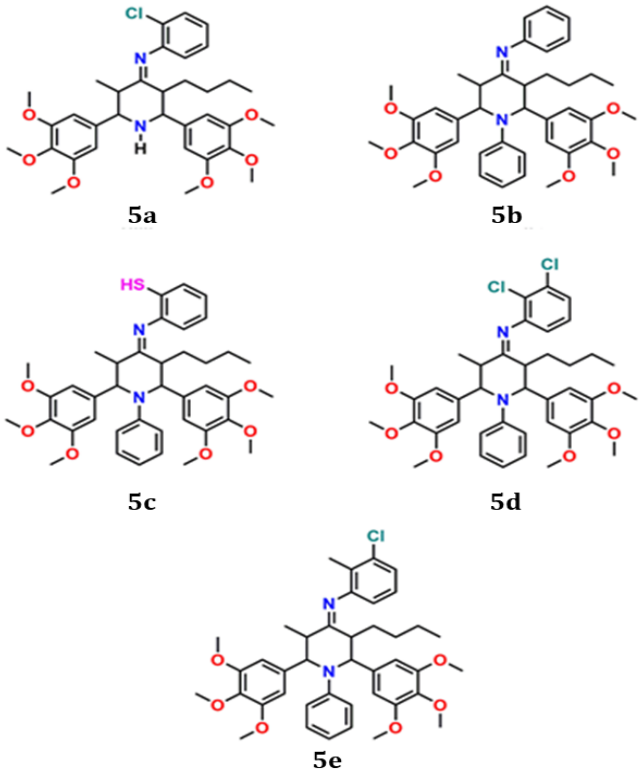

Chart 1. Molecular structure of Piperidin-4-imines (5a-e).

For the synthesized molecules, the ground state structures were optimized by density functional theory with basis set of b3lyp 6-31g (d,p) in Gaussian 09 program.[26,27] Using this theory, electronic transitions, and the charge transfers in molecular systems, frontier molecule orbitals (FMOs)are calculated as shown in **Fig.2.**

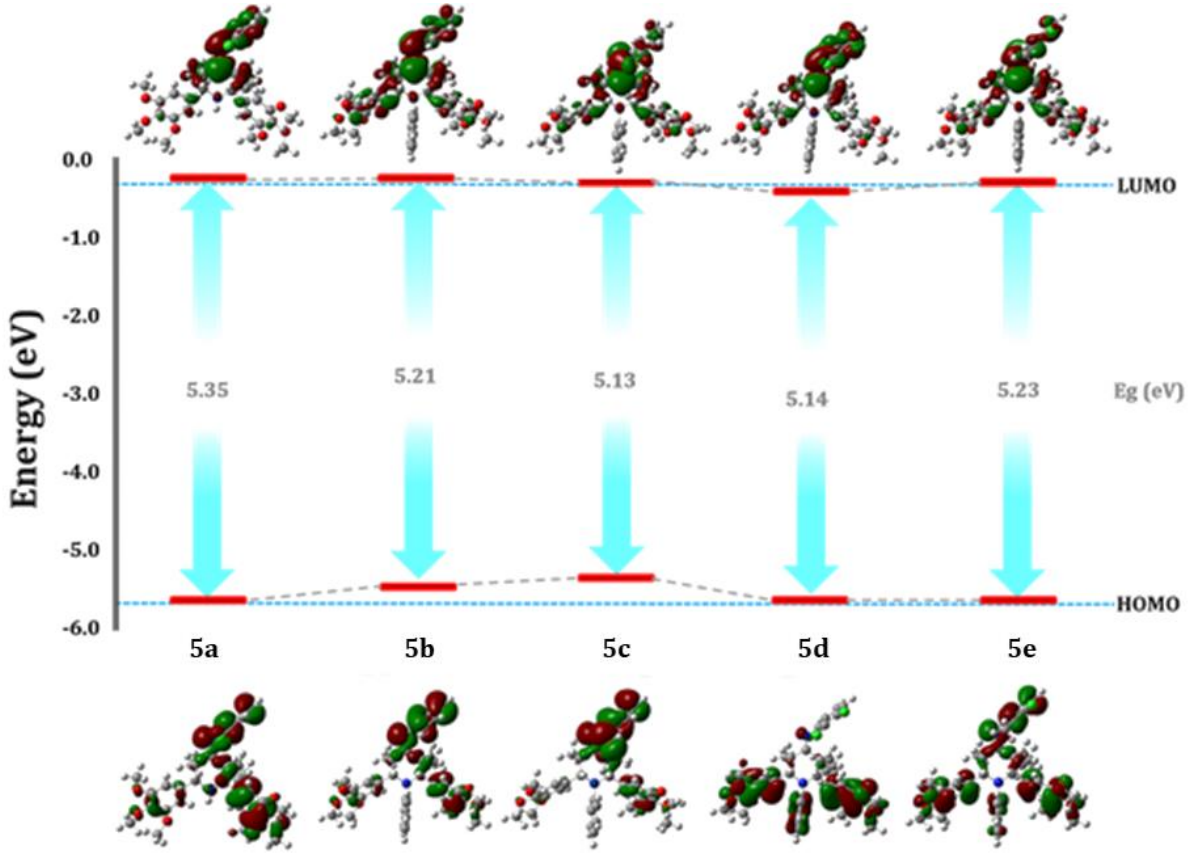

Fig. 2. DFT-optimized Frontier molecular orbitals and HOMO-LUMO energy gaps for Piperidine-4-imines (5a-e).

Based on the highest occupied molecular orbital (HOMO) and the lowest unoccupied molecular orbital (LUMO) energy values, some quantum mechanical descriptors such as energy band gap energy (E_{HOMO}-E_{LUMO}), ionization potential (I=-E_{HOMO}), electron affinity (A=-E_{LUMO}), chemical hardness(η= (I-A)/2), chemical softness(ζ=1/2η), electronegativity (χ(I+ A)/2), chemical potential (μ=-(I+A)/2), electrophilicity index (ω=μ^2/2η), and maximum charge transfer index (ΔN_{max}.=-μ/η)for the compounds **5a-c** were calculated and summarized in **Table 1.**

Table 1. Energy band gapvalues and other quantum mechanical descriptors of the compounds 5a-e.

Quantum mechanical descriptors (eV)	5a	5b	5c	5d	5e
Band gap energy (E_{HOMO}-E_{LUMO})	5.35	5.21	5.13	5.14	5.23
Ionization potential (I=-E_{HOMO})	5.65	5.63	5.43	5.64	5.51
Electron affinity (A=-E_{LUMO}),	0.39	0.45	0.40	0.58	0.30
Chemical hardness (η= (I-A)/2)	2.63	2.59	2.51	2.53	2.60
Chemical softness (ζ=1/2η)	0.19	0.19	0.20	0.20	0.19

Electronegativity (χ=(I+A)/2),	3.02	3.04	2.91	3.11	2.90
Chemical potential (μ=-(I+A)/2)	-3.02	-3.04	-2.91	-3.11	-2.90
Electrophilicityindex ($\omega=\mu^2/2\eta$)	1.73	1.78	1.68	1.91	1.61
Maximum charge transfer index ($\Delta N_{max}.=-\mu/\eta$)	1.14	1.17	1.15	1.22	1.11

The molecular electrostatic potential (MEP) is a highly important descriptor to understand the electrophilic and nucleophilicsitesin molecular structure. In MEP mapping system, sixdifferent colors are observed,such as red, orange, yellow, green, cyan, and blue.The red colour of map is the highly electron-rich region, while the blue colour is the extremely poor electron or electron-deficient region of the molecule. The decreasing order of electrostatic potential colour isblue>cyan>green> yellow> orange> red. The observed negative sites to positive electrostatic potential values are-4.656e^{-2} and +4.656e^{-2} for **5a**; -4.885e^{-2} and +4.885e^{-2} for **5b**; -5.068e^{-2} and +5.068e^{-2} for **5c**; -4.331e^{-2} and +4.331e^{-2} for **5d**; and -4.329e^{-2} and +4.329e^{-2} for **5e**compounds with B3LYP functional and 6–31g (d,p) basis set as illustrated in **Fig. 3.**

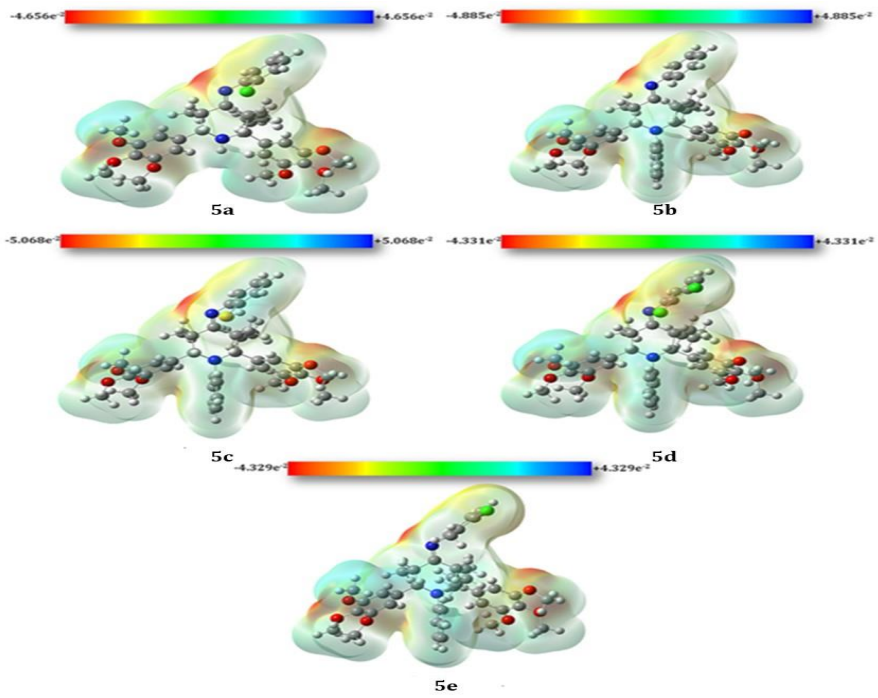

Fig. 3. The MEP surfaces of Piperidin-4-inmines (5a-e).

In the present study, the negative regions are concentrated over the methoxy groups and imine moiety for all the compounds; on the other hand, the positive regions are located over hydrogen atoms in the alkyl chains and phenyl moieties. The obtained results clearly suggested that the high electronegativity of the methoxy moieties and imine units makes it the most reactive part of the all compounds for docking studies.

4. Structure of the SARS-CoV-2

The SARS-CoV-2 belongs to a spherical β-coronavirus family and also pleomorphic in nature. The coronavirus structure[28] is composed of the following structural fragments, viz.(i) spike proteins (S), (ii) membrane proteins (M), (iii) envelope proteins (E), (iv) nucleocapsid (N), and (v) hemagglutinin-aserase dimer (HE) glycoproteins along with

RNA as genetic material. As shown in **Fig.4.** The 'S' protein peripheral surface sites resemble a crown shape in an electron microscope. The SARS-CoV-2 nucleotide is resembled as 80, 55, and 50% homolog to SARS-CoV-1, MERS, and common cold CoV, respectively.

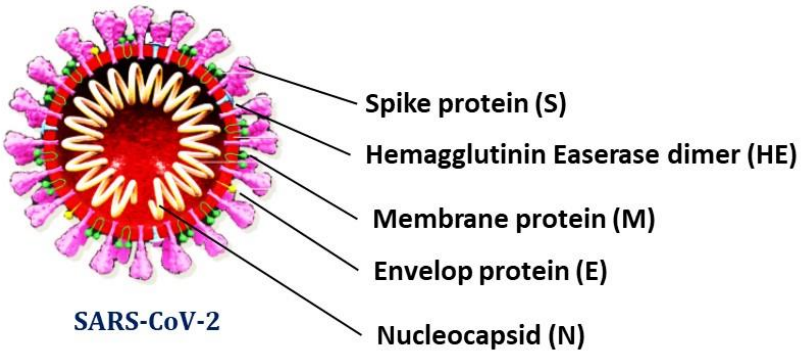

Fig. 4. Structure of SARS-CoV-2.

The SARS-CoV-2 spike protease's mechanistic action against the human cell

A brief mechanistic pathway of the SARS CoV-2 'S' protein against humans is facilitated by the ACE2 biomolecule, which acts as a human entry receptor. Based on the sequence alignment results, the spike-receptor binding domain (RBD) sequences of the SARS-CoV-2 and the SARS-CoV are 76% analogous. Therefore, the SARS-CoV-2 easily binds to the ACE2 receptor.However, the pathogenic causing SARS-CoV-2 virus can be prevented by many pathways as follows:(i) the target viral enzyme proteins act as a blocker for virus RNA synthesis and replication, (ii) preventing viral entry to human cell ACE2 receptors; (iii) some of the virulence elements are generated to restore the innate host immunity, and (iv) specific receptors present in the host may prevent the virus entry into the host cells.Theinteractions between the virus and host cells that ACE2 binding site of antiviral drugs molecular design have to stop the 'S' protein physicochemical activities. Otherwise, TMPRSS2 protease, neuropilin-1, and interfaces of heptad repeat-1 and heptad repeat-2 domains might be in critical state. Thus, the molecular protein biology relationship is strongly limited in the beginning stage to prevent the novel coronavirus and its mutations.

5. Molecular docking study

In the modern drug discovery programs, molecular docking analysis of small molecules in the protein or receptor binding sites is carried out by computational technique. Herein, four different kinds of receptors of SARS CoV-2 (6lu7 protease) and its mutations (delta variant;7w92 protease, delta plus variant; tnx7 glycoprotease, and omicrom;7s0b protease] were used in moleculardocking studies throughAutoDockVina software program[29] as shown in **Table 2.**

Table 2. Molecular docking scores of piperidin-4-imines(5a-e) for SARS CoV-2 and its mutation proteases

Compound	6lu7 protease		7w92 protease		7nx7glycoprotease		7s0b	
	Binding energy (kcal/mol)	Inhibition constant (µM)	Binding energy (kcal/mol)	Inhibition constant (µM)	Binding energy (kcal/mol)	Inhibition constant (µM)	Binding energy (kcal/mol)	Inhibition constant (µM)
5a	**-6.6**	**14.3482**	-6.2	28.2048	-5.9	46.8241	**-6.6**	**14.3482**
5b	-6.1	33.3969	-6.2	28.2048	-5.6	77.7347	-6.5	16.9894
5c	-5.8	55.4436	-6.0	39.5446	-6.2	28.2048	-5.9	46.8241
5d	-6.4	20.1168	**-6.3**	**23.8200**	-6.2	28.2048	-6.4	20.1168
5e	-6.2	28.2048	**-6.3**	**23.8200**	**-6.4**	**20.1168**	-6.5	16.9894

In molecular docking analysis, nine different poses were obtained for **5a-e** compounds. The obtained root mean square deviation lower bound and upper bound valuesare2 Å nearly;hence, the value is agreeable and reliable in molecular docking studies (SI).Furthermore,the inhibition constants were determined using K_i=exp(ΔG/RT) equation for **5a-e** compounds, where ΔG, R, and Tare the docking binding energy, gas constant (1.9872036×10^3 kcal/mol), and room temperature (298.15 K), respectively.All the covalent and non-covalent bonding interactions (SI, Table 1) for the protein 6lu7 protease, 7w92 protease, 7nx7 glucoprotease, and 7s0b protease were determined for Piperidin-4-imines (**5a-e**).

As can be seen in**Table2**, the highest molecular docking score having SARS CoV-2 and its mutations of 2D and 3D protein-lead molecular interactions graphics are shown in **Fig. 4.**

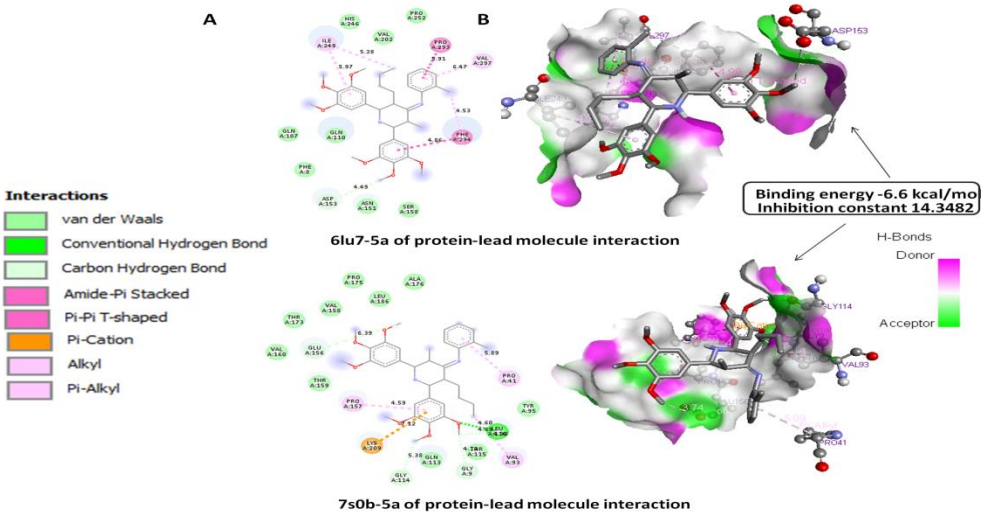

Fig 4(i) 6lu7 & 7s0b protein-lead molecule interaction of 5a

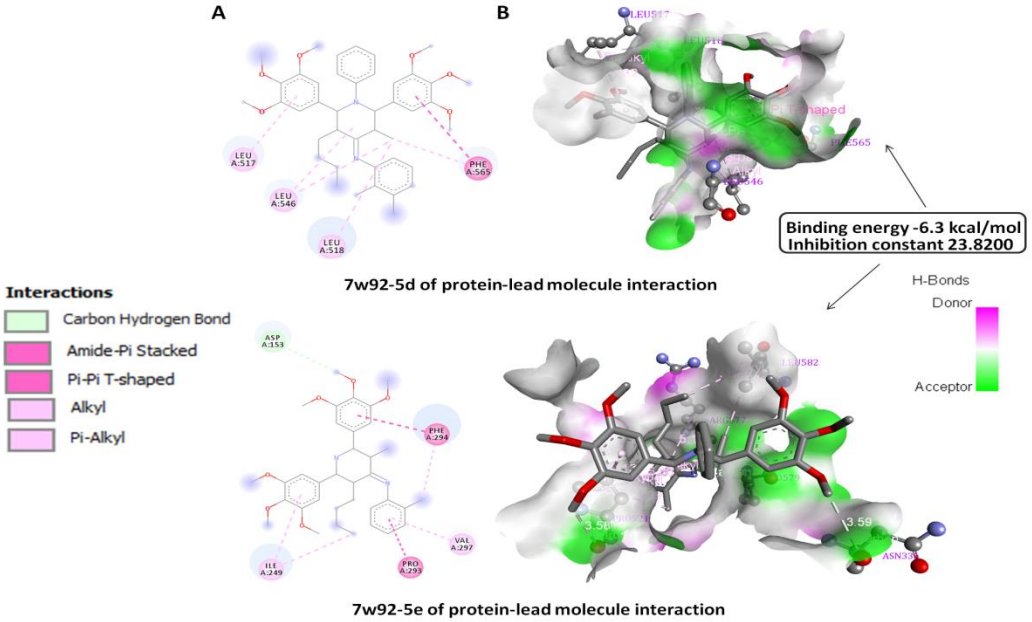

Fig 4(ii) 7w92 protein-lead molecule interactions of 5d and 5e

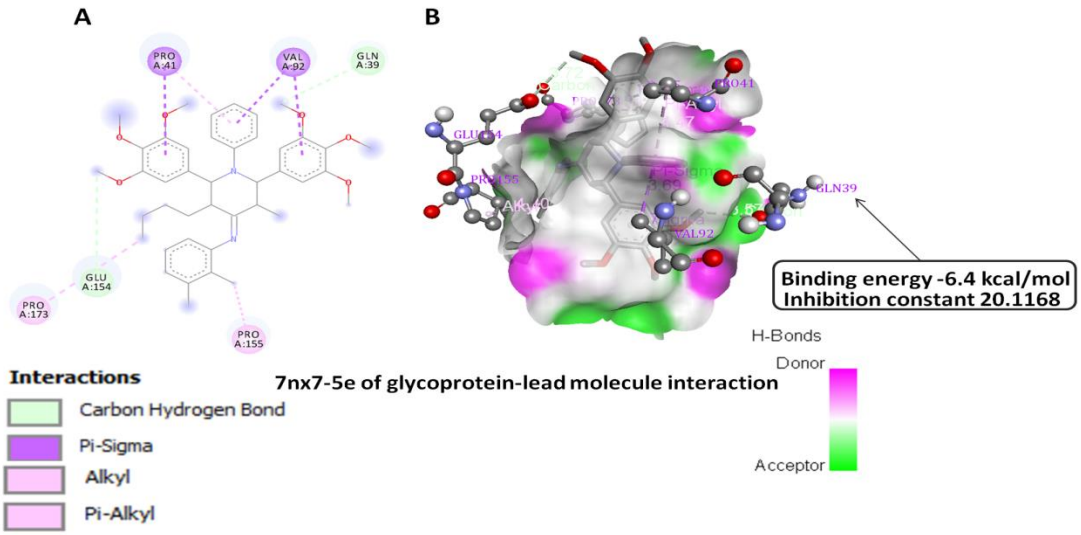

Fig 4(iii) 7nx7 protein-lead molecule interactions of 5e

The best affinitybinding energy was calculatedfor **5a [Fig-4(i)]**compound against **6lu7protease** as-6.6 kcal/molwith a corresponding inhibition constant of 14.3482μM.(i). One carbon hydrogen bond with a distance of 3.78 Å was observed between H-donor of $–OCH_3$ and H-acceptor of ASP153 amino acid residue. ii). Two π-hydophobic interactions, such as π-π T-shaped and amide-π stacked, were observed with distance of 4.99 (between π-orbital of trimethoxy substituted 'A' phenyl ring and of π-orbital of PHE294 amino acid) and 4.03 Å(between amide carbonyl carbon [PRO294:Camino acid residue and PHE294:Namino acid residue]),respectively. (iii).One alkyhydrophobic interaction with a distance of 4.7Å between long alkyl chain of butyl group and branched alkyl chain of ILE249 residue. (iv). Four π-alky interactions between (a) π-orbital of trimethoxy substituted 'B' phenyl ring and branched alkyl chain of ILE249 amino acid residue (bond distance: 5.22 Å), (b) π-orbital of PHE294 amino acid residue and chlorophenyl moiety (4.86 Å), (c) π-orbital of chlorophenyl and cyclic alkyl chain of PRO293 amino acid residue (5.48 Å), and (d) π-orbital of chlorophenyl and branched alkyl chain of VAL297 amino acid residue (4.91 Å).

In the case of **7w92 protease**, **5d** and **5e [Fig.4(ii)]** exhibit good potentials and also identical affinity binding energy and (-6.3 kcal/mol) with an inhibition constant of 23.8200 μM than that of **5a**(-6.2 kcal/mol, and 28.2048 μM), **5c**(-6.0 kcal/mol, and 39.5446 μM), and **5e**(-6.2 kcal/mol and 28.2048 μM) compounds.The**5d** compounds have one π-π T-shaped, threealky-alkyl, and two π-alkyl interactions. For example, (i) the π-π T-shaped alkyl-alkyl has a bond distance of 4.93 Å between π-orbital of trimethoxy substituted 'A' phenyl ring and π-orbital of PHE565 amino acid residue. (ii) Three alky-alkyl interactions have a bond distance of 5.17 (between methyl moiety of piperidine and branched alkyl chain of LEU518 amino acid residue), 5.08 (between methyl moiety of piperidine and branched alkyl chain of LEU546 amino acid residue), and 4.85 Å (between branched alkyl chain of LEU546 amino acid residue and cyclic piperidine chain).(iii) Two π-alkyl interactions consist of a bond distance of 5.32 Å (between π-orbital of trimethoxy substituted 'B' phenyl ring and branched alkyl chain LEU517 amino acid residue) and 4.11 Å (between π-orbital ofPHE565 amino acid residue and methyl moiety of piperidine unit).

Similarly, (i) the **5e**compounds have three carbon hydrogen bonds with distance of 3.59 (between H-donor of $–OCH_3$ group and H-acceptor of carbonyl oxygen ASN331 amino acid residue), 3.58 (between H-donor of $–OCH_3$ group and H-acceptor of carbonyl oxygen PRO521 residue), and 3.54 Å (between H-donor of PRO579 amino acid residue and H-acceptor of imine nitrogen moiety).Also, (ii) the **5e**compoundscontain four alkyl–hydrophobic

interactions between, such as (a) methyl chain of piperidine and branched alkyl chain of LEU582 amino acid residue (bond distance: 4.95 Å), (b) linear butyl chain of piperidine and branched alkyl chain of LEU582 amino acid residue (bond distance: 4.58 Å), (c) branched alkyl chain of PRO521amino acid residue and methyl moiety of chloromethylphenyl unit (4.38 Å), and (d) methyl moiety of chloromethylphenyl unit and cyclic piperidine unit (5.36 Å). Additionally, (iii) the **5e** compounds have three π-alkyl interactions, namely(a)π-orbital of chloromethylphenyl moiety and linear alkyl chain of ARG577 amino acid residue (5.16 Å), (b) π-orbital of chloromethylphenyl moiety and cyclic alkyl chain of PRO521 amino acid residue (5.04 Å), and (c) π-orbital of trimethoxy substituted 'B' phenyl ring and cyclic alkyl chain of PRO521 amino acid residue (bond distance: 4.15 Å).

For **7nx7glycoprotease,** the **5e[Fig-4(iii)]**compound show better affinity binding score of -6.4 kcal/mole with20.1168μM inhibition constant due to two carbon hydrogen bonds, two alkyl–alkyl hydrophobic, three π-σ hydrophobic, and one π-alkyl hydrophobic interactions.For example, (i) two carbon hydrogen bonds have a bond distance of 3.72 (between H-donor of methoxy moiety from 'B' ring and carbonyl oxygen moiety of GLU154 amino acid residue) and 3.57 Å (between H-donor of methoxy moiety from 'A' ring and carbonyl oxygen moiety of amide carbonyl oxygen moiety of GLN39 amino acid residue), (ii) two alkyl–alkyl hydrophobic interactions with abond distance of 4.80 (between methyl moiety of chloromethylphenyl ring and cyclic alkyl chain of PRO155 amino acid residue) and 4.39 Å (between linear butyl chain of piperidine moiety and cyclic alkyl chain of PRO173 amino acid residue),(iii) three π-σ hydrophobic interactions with abond distance of 3.85 (between cyclic CH moiety of PRO41 amino acid residue and π-orbital of trimethoxy substituted 'B' phenyl ring), 3.71 (between open chain CH moiety of VAL92 amino acid residue and π-orbital of trimethoxy substituted 'A' phenyl ring) and 3.69 Å and (iv)one π-alkyl hydrophobic interaction of a bond distance of 4.46 Å (between cyclic alkyl chain of PRO41 amino acid residue and π-orbital of N-phenyl moiety).

Likewise, the **5a** compounds exhibit the best affinity binding score of -6.6 kcal/mole with a14.3482μM inhibition constant against **omicron 7s0b protease**.For example, one hydrogen bonding interaction of a distance of 1.91 Å betweenH-Donor of LEU116:HN amino acid residue and H-Acceptor of trimethoxy substituted 'B' phenyl ring, two electrostatic interaction of a π-cation with a bond distance of 4.56 (between positive charge of LYS209:NZ amino acid residue and π-orbital of trimethoxy substituted 'A' phenyl ring) and a π-anion with a bond distance of 4.19 Å (between negative charge of A:GLU156:OE_2amino acid residue and π-orbital of chlorophenylring), and two π-alkyl interactions with distance of 5.01 (betweenπ-orbital of chlorophenyl ring and cyclic alkyl chain of PRO41 amino acid residue) and 4.96 Å (between π-orbital of trimethoxy substituted 'A' phenyl ring and cyclic alkyl chain of PRO157 amino acid residue).

6. Drug-likeness properties

The drug-likeness properties were analyzed by molinspiration servers where Lipinski's rule states that orally active drug must satisfy the following five criteria: (i) molecular weight, (ii) log, (iii) hydrogen bond donor, (iv) hydrogen bond accepter, and (v) total polar surface area for the synthesis piperdine-4-imines of 5a-e as depicted in **Table 3**.

Table 3. The drug-likeness properties of piperdine-4-imines of **5a-e**.

Piperidin-4-imines	[a]MW (<500Da)	[b]LogP (<5.6)	[c]HBD (<5)	[d]HBA (<10)	[e]TPSA (<140Å)
5a	611.18	7.71	1	8	79.80
5b	701.30	9.12	0	8	71.01
5c	684.90	8.79	0	8	71.01
5d	721.72	9.19	0	8	71.01
5e	652.83	8.70	0	8	71.01
[a]MW—Molecular weight,[b]LogP—octanol/water partition coefficient,					

[c]HBD—Hydrogen bond donor, [d]HBA—Hydrogen bond acceptor, and e TPSA—Total polar surface area.

An orally active drug has to satisfy Lipinski's rule without violation of the following standards:(i) the lipophilicity or octanol/water partition coefficient (LogP) of a molecule should not be greater than 5, (ii) molecular weight of the compound must be 500 Da, (iii) the hydrogen bond donor should not be more than 5 and hydrogen bond accepter should not be more than 10, and (iv) the total molecular polar surface must be greater or equal 140 Å. The addition of an oral drug can be absorbed TPSA value when it is greater than 60 Å. Hydrogen bonding correlation is significant for the bioactivity of **5a-e** piperidin-4-imines. The above obtained results clearly suggest that the designed and synthesized lead molecule violates molecular weight and LogPvalues alone. Also, Lipinski's rule does not predict if these compounds are pharmacologically active. Therefore, these lead molecules may have better change to use in the invitro level analysis for SARS CoV-2 and its mutations.

7. Spectral data of compounds 5a-5e

7.1(Z)-3-butyl-N-(2-chlorophenyl)-5-methyl-2,6-bis(3,4,5-trimethoxyphenyl)piperidin-4-imine (5a)

Yield: 78%; m.p: 173–174°C, IR (KBr) (cm^{-1}): 3302 (N-H stretching), 2933 (aromatic C-H stretching), 1697 (C=C stretching), 1590 (N-H bending) 1342 (C-O stretching), 1231 (C-N stretching), 827 (C-Cl stretching), 707 (C-H out of plan bending), 675 (N-H wagging). ^{1}H NMR(400MHz,DMSO):δ7.02(m,ArH),3.7(s,OCH_3),2.83.0(m,CH_2),2.6(s,NH),0.8(t,CH_3).^{13}CNMR(400MHz,DMSO):11.34,14.36,22.63,29.80,39.34,40.18,51.71,72.14,105.55,137.15,153.13,210.85.

7.2(Z)-3-butyl-5-Methyl-N,1-diphenyl-2,6-bis(3,4,5-trimethoxyphenyl)piperidin-4-imine(5b)

Yield: 72%; m.p: 171–175°C, IR (KBr) (cm^{-1}): 3310 (N-H stretching), 2937 (aromatic C-H stretching), ,1698 (C=C stretching), 1592 (N-H bending) 1341 (C-O stretching), 1234 (C-N stretching), 828 (C-Cl stretching), 709 (C-H out of plan bending), 676 (N-H wagging). ^{1}H NMR(400MHz,DMSO):7.01(m,ArH),3.08(s,OCH_3),2.81.0(m,CH_2),2.03(s,NH),0.81(t,CH_3).^{13}CNMR(400MHz,DMSO):11.35,14.46,21.63,22.80,40.34,41.18,52.71,72.14,105.55,138.15,153.55,210.87.

7.3(Z)-2-((3-butyl-5-methyl-1-phenyl-2,6-bis(3,4,5-trimethoxyphenyl)piperidin-4-ylidene)amino)benzenethiol(5c)

Yield: 69%; m.p: 176–179°C, IR (KBr) (cm^{-1}): 3311 (N-H stretching), 2933 (aromatic C-H stretching), 1694 (C=C stretching), 1591 (N-H bending) 1342 (C-O stretching), 1233 (C-N stretching), 827 (C-Cl stretching), 706 (C-H out of plan bending), 677 (N-H wagging). ^{1}H NMR(400MHz,DMSO):7.03(m,ArH),3.09(s,OCH_3),2.82.0(m,CH_2),2.04(s,NH),0.82(t,CH_3).^{13}CNMR(400MHz,DMSO):11.36,14.47,21.64,22.81,40.32,41.17,52.72,72.13,105.56,138.16,153.57,210.88.

7.4(Z)-3-butyl-N-(2,3-dichlorophenyl)-5-methyl-1-phenyl-2,6-bis(3,4,5-trimethoxyphenyl)piperidin-4-imine(5d)

Yield: 68%; m.p: 171–173°C, IR (KBr) (cm^{-1}): 3314 (N-H stretching), 2931 (aromatic C-H stretching), 1695 (C=C stretching), 1593 (N-H bending) 1343 (C-O stretching), 1234 (C-N stretching), 828 (C-Cl stretching), 707 (C-H out of plan bending), 674 (N-H wagging). ^{1}H NMR(400MHz,DMSO):7.05(m,ArH),3.04(s,OCH_3),2.81.0(m,CH_2),2.08(s,NH),0.83(t,CH_3).^{13}CNMR(400MHz,DMSO):11.32,14.41,21.64,22.83,40.33,41.14,52.75,72.14,105.57,138.17,153.54,210.81.

7.5(Z)-3-butyl-N-(3-chloro-2-methylphenyl)-5-methyl-1-phenyl-2,6-bis(3,4,5-trimethoxyphenyl)piperidin-4-imine(5e)

Yield: 74%; m.p: 178–180°C, IR (KBr) (cm^{-1}): 3311 (N-H stretching), 2934 (aromatic C-H stretching), 1692 (C=C stretching), 1595 (N-H bending) 1341 (C-O stretching), 1233 (C-N stretching), 821 (C-Cl stretching), 708 (C-H out of plan bending), 675 (N-H wagging). ^{1}H NMR(400MHz,DMSO):7.04(m,ArH),3.01(s,OCH_3),2.82.0(m,CH_2),2.01(s,NH),0.85(t,CH_3).^{13}CNMR(400MHz,DMSO):11.31,14.42,21.61,22.87,40.31,41.15,52.77,72.11,105.58,138.18,153.51,210.83.

8. Conclusion

In this summary, we would conclude that we have successfully synthesized 5 piperidin-4-imines compounds by condensation and cyclisation of aldehyde and ketone by following the Schiff base method. The electronic configuration of HOMO and LUMO had revealed that methoxy and imine units are themost reactive parts of the synthesized compounds. Similarly, molecular docking studies of SARS CoV-2 receptors and its four protease (6lu7, 7w92, tnx7 and 7s0b) were calculated for title compounds. Among these compounds,**5a** ,**5d** and **5e** exhibited best binding energy and inhibition constant. The results of the drug-likeness properties also exposed that the title of the compounds violate only weight and LogP value. From all theseobservations, we conclude that piperidin-4-imines doeshave the ability to inhibit SARS Covid-2 in host cell.However, additional in vitroresearchand in vivo research are necessary to verify the results.

9. References

1. World Health Organization (WHO). Pneumonia of unknown cause – China. Geneva: WHO; 2020. Available from: https://www.who.int/csr/don/05-january-2020-pneumonia-of-unkown-cause-china/en/
2. Huang C, Wang Y, Li X, Ren L, Zhao J, Hu Y, et al. Clinical features of patients infected with 2019 novel coronavirus in Wuhan, China. Lancet. 2020;S0140-6736(20)30183-5. https://doi.org/10.1016/S0140-6736(20)30154-9 PMID: 31986261
3. World Health Organization (WHO). WHO Director-General's remarks at the media briefing on 2019-nCoV on 11 February 2020. Geneva: WHO; 2020. Available from: https://www.who.int/dg/speeches/detail/who-director-general-s-remarks-at-the-media-briefing-on-2019-ncov-on-11-february-2020
4. Huang C, Wang Y, Li X, Ren L, Zhao J, Hu Y, Zhang L, Fan G, Xu J, Gu X, Cheng Z. Clinical features of patients infected with 2019 novel coronavirus in Wuhan, China. The lancet. 2020 Feb 15;395(10223):497-506.
5. Alimohamadi Y, Sepandi M, Taghdir M, Hosamirudsari H. Determine the most common clinical symptoms in COVID-19 patients: a systematic review and meta-analysis. Journal of preventive medicine and hygiene. 2020 Sep;61(3):E304.
6. Centers for Disease Control and Prevention (CDC). Coronavirus Disease 2019 (COVID-19). Atlanta: CDC; 2020. Available from: https://www.cdc.gov/coronavirus/2019-ncov/about/symptoms.html
7. Wu YC, Chen CS, Chan YJ. Overview of the 2019 novel coronavirus (2019-nCoV): The pathogen of severe specific contagious pneumonia (SSCP). J Chin Med Assoc. 2020; [Epub ahead of print]. https://doi.org/10.1097/JCMA.0000000000000270 PMID: 32049687
8. Li MY, Li L, Zhang Y, Wang XS. Expression of the SARS-CoV-2 cell receptor gene ACE2 in a wide variety of human tissues. Infectious diseases of poverty. 2020 Apr 1;9(02):23-9.
9. Rahman FI, Ether SA, Islam MR. The "Delta Plus" COVID-19 variant has evolved to become the next potential variant of concern: mutation history and measures of prevention. Journal of Basic and Clinical Physiology and Pharmacology. 2022 Jan 1;33(1):109-12.
10. Kumar A, Parashar R, Kumar S, Faiq MA, Kumari C, Kulandhasamy M, Narayan RK, Jha RK, Singh HN, Prasoon P, Pandey SN. Emerging SARS-CoV-2 variants can potentially break set epidemiological barriers in COVID-19. Journal of Medical Virology. 2022 Apr;94(4):1300-14.
11. Mohapatra RK, Sarangi AK, Kandi V, Azam M, Tiwari R, Dhama K. Omicron (B. 1.1. 529 variant of SARS-CoV-2); an emerging threat: current global scenario. Journal of medical virology. 2022 May;94(5):1780-3.
12. Li G, De Clercq E. Therapeutic options for the 2019 novel coronavirus (2019-nCoV). Nature reviews Drug discovery. 2020 Mar;19(3):149-50.
13. Yao X, Ye F, Zhang M, Cui C, Huang B, Niu P, Liu X, Zhao L, Dong E, Song C, Zhan S. In vitro antiviral activity and projection of optimized dosing design of hydroxychloroquine for the treatment of severe acute respiratory syndrome coronavirus 2 (SARS-CoV-2). Clinical infectious diseases. 2020 Jul 28;71(15):732-9.
14. Wang Y, Fan G, Salam A, Horby P, Hayden FG, Chen C, Pan J, Zheng J, Lu B, Guo L, Wang C. Comparative effectiveness of combined favipiravir and oseltamivir therapy versus oseltamivir monotherapy in critically ill patients with influenza virus infection. The Journal of infectious diseases. 2020 Apr 27;221(10):1688-98.
15. Taniguchi H, Ebina M, Kondoh Y, Ogura T, Azuma A, Suga M, Taguchi Y, Takahashi H, Nakata K, Sato A, Takeuchi M. Pirfenidone in idiopathic pulmonary fibrosis. European Respiratory Journal. 2010 Apr 1;35(4):821-9.

16. Zhu Z, Lu Z, Xu T, Chen C, Yang G, Zha T, Lu J, Xue Y. Arbidol monotherapy is superior to lopinavir/ritonavir in treating COVID-19. Journal of Infection. 2020 Jul 1;81(1):e21-3.
17. Zhu M, Zhou H, Ma L, Dong B, Zhou J, Zhang G, Wang M, Wang J, Cen S, Wang Y. Design and evaluation of novel piperidine HIV-1 protease inhibitors with potency against DRV-resistant variants. European Journal of Medicinal Chemistry. 2021 Aug 5;220:113450.
18. Rajput, A. P., and D. V. Nagarale. "Synthesis, characterization and antimicrobial study of piperidine-2, 6-diones derivatives." Pharm. Chem 8 (2016): 182-186.
19. Khanum SA, Girish V, Suparshwa SS, Khanum NF. Benzophenone-N-ethyl piperidine ether analogues—Synthesis and efficacy as anti-inflammatory agent. Bioorganic & medicinal chemistry letters. 2009 Apr 1;19(7):1887-91.
20. Kankala S, Kankala RK, Balaboina R, Thirukovela NS, Vadde R, Vasam CS. Pd-N-heterocyclic carbene catalyzed synthesis of piperidine alkene–alkaloids and their anti-cancer evaluation. Bioorganic & medicinal chemistry letters. 2014 Feb 15;24(4):1180-3.
21. Carroll FI, Dolle RE. The Discovery and Development of the N-Substituted trans-3, 4-Dimethyl-4-(3′-hydroxyphenyl) piperidine Class of Pure Opioid Receptor Antagonists. ChemMedChem. 2014 Aug;9(8):1638-54.
22. Lei, Peng, Xuebo Zhang, Yan Xu, Gaofei Xu, Xili Liu, Xinling Yang, Xiaohe Zhang, and Yun Ling. "Synthesis and fungicidal activity of pyrazole derivatives containing 1, 2, 3, 4-tetrahydroquinoline." Chemistry Central Journal 10, no. 1 (2016): 1-6.
23. Lv K, Tao Z, Liu Q, Yang L, Wang B, Wu S, Wang A, Huang M, Liu M, Lu Y. Design, synthesis and antitubercular evaluation of benzothiazinones containing a piperidine moiety. European Journal of Medicinal Chemistry. 2018 May 10;151:1-8.
24. Konwar M, Sarma D. Advances in developing small molecule SARS 3CLpro inhibitors as potential remedy for corona virus infection. Tetrahedron. 2021 Jan 1;77:131761.
25. Cannalire R, Cerchia C, Beccari AR, Di Leva FS, Summa V. Targeting SARS-CoV-2 proteases and polymerase for COVID-19 treatment: state of the art and future opportunities. Journal of medicinal chemistry. 2020 Nov 13;65(4):2716-46.
26. Casida ME, Chong DP, editors, Recent developments in density functional theory. Singapore: World Scientific; 1995;1:155–192.
27. Casida ME, Casida KC, Salahub DR. Excited-state potential energy curves from time-dependent density-functional theory: a cross section of formaldehyde's1A1 manifold. Int. J. Quantum Chem.1998;70:933–941.
28. Vankadari N. Structure of furin protease binding to SARS-CoV-2 spike glycoprotein and implications for potential targets and virulence. The journal of physical chemistry letters. 2020 Jul 28;11(16):6655-63.
29. Trott O, Olson AJ (2010) AutoDockVina: improving the speed and accuracy of docking with a new scoring function, efficient optimization, and multithreading. J ComputChem 31: 455-461. 1
30. Patil, Anil Kumar, and Sharanappa Godi Ganur. "Comparative study on the effect of nano additives with biodiesel blend on the performance and emission characteristics of a laboratory ci engine." International journal of mechanical and production engineering research and development (ijmperd) ISSN (p): 2249-6890.
31. Al-Fatlawi, A. L. A. A. H. U. S. A. E. E. N. "Effects of chlorine dioxide and some water quality parameters on the formation of THMs in water treatment plants." International Journal of Civil, Structural, Environmental and Infrastructure Engineering Research and Development (IJCSEIERD) 4.2 (2014): 73-86.
32. DOSH, RUKIA JABER, et al. "Energy and some atomic properties for excited state of AR ion using Hartree-Fock method." International Journal of Mechanical and Production Engineering Research and Development 8.6 (2018): 827-830.
33. Nandhini, D., S. Subashchandrabose, and P. RAMESH. "Synthesis, characterization and computation of potassium doped calcium hydroxide nanoparticles and nanotubes." International Journal of Mechanical and Production Engineering Research and Development (IJMPERD) 9.1 (2019): 441-448.
34. Benmekhbi, L., et al. "Inhibition Study By Molecular Docking Of Dihydrofolate Reductase Of Escherichia Coli With Some Chalcone Molecules." International Journal of Applied, Physical and Bio-Chemistry Research 4.6 (2014): 17-24.
35. Singh, Neha, et al. "Awareness Towards Covid-19 Pandemic among Farm Women and its Technological Strategies." International Journal of Agricultural Science and Research (IJASR) 10 (2020): 151-158.